

## **NOTICE CONCERNING COPYRIGHT RESTRICTIONS**

This document may contain copyrighted materials. These materials have been made available for use in research, teaching, and private study, but may not be used for any commercial purpose. Users may not otherwise copy, reproduce, retransmit, distribute, publish, commercially exploit or otherwise transfer any material.

The copyright law of the United States (Title 17, United States Code) governs the making of photocopies or other reproductions of copyrighted material.

Under certain conditions specified in the law, libraries and archives are authorized to furnish a photocopy or other reproduction. One of these specific conditions is that the photocopy or reproduction is not to be "used for any purpose other than private study, scholarship, or research." If a user makes a request for, or later uses, a photocopy or reproduction for purposes in excess of "fair use," that user may be liable for copyright infringement.

This institution reserves the right to refuse to accept a copying order if, in its judgment, fulfillment of the order would involve violation of copyright law.

## High Temperature Field Testing of Polyphenylenesulphide Composite Coatings

Toshifumi Sugama<sup>1</sup>, Paul Hirtz<sup>2</sup> and Keith Gawlik<sup>3</sup>

<sup>1</sup>Brookhaven National Laboratory

<sup>2</sup>Thermochem, Inc.

<sup>3</sup>National Renewable Energy Laboratory

### Keywords

*Corrosion, scaling, O&M, heat exchangers, carbon steel, geothermal fluids, coating systems*

### ABSTRACT

Researchers at Brookhaven National Laboratory, Thermochem, Inc., and the National Renewable Energy Laboratory, completed short-term tests in a high temperature environment of polymer-based coating systems intended to reduce the capital equipment and maintenance costs of heat exchangers and other process equipment operating in corrosive and fouling geothermal applications. These coating systems act as barriers to corrosion, protecting low-cost carbon steel tubing and are formulated to resist wear from hydroblasting and to have high thermal conductivity. Polymer composite systems applied to coupons and the interiors of heat exchanger tubes were exposed to injection geothermal fluid over a temperature range of 392°F (200°C) to 180°F (82°C) for four weeks at the Puna Geothermal Venture power plant with uncoated carbon steel and stainless steel tubes as controls. Analyses of the exposed coatings showed that scale adhesion to the coating was weak in comparison to the adhesion to uncoated materials and that the coating resisted attack from the high temperature fluid. Disbonding of the coating was observed in the commercially-coated heat exchanger tubes. A mechanism related to the method used in the coating application has been identified for the failure.

### Introduction

Corrosion, erosion, and fouling by scale deposits are major issues for geothermal-fluid-wetted process equipment at several facilities. In some cases, expensive, corrosion-resistant alloys are used in heat exchangers, pipelines, and other equipment because of the need for corrosion resistance. In other cases, frequent heat exchanger re-tubing, pipeline repair and replacement, or other maintenance work is required to repair

scaled and corroded components. Capital and maintenance costs of geothermal process equipment could be reduced considerably if inexpensive carbon steel could be coated with a low-cost barrier coating that provides corrosion resistance equal to that of high-grade alloy steels with thermal and mechanical properties tailored for the application through the use of different filler materials. Thus, corrosion-, erosion-, and fouling-resistant coatings for carbon steel tubes are being investigated at Brookhaven National Laboratory (BNL) and the National Renewable Energy Laboratory, in cooperation with industry partners Puna Geothermal Venture (PGV) and Thermochem, Inc. (TCI).

The research program found that polyphenylenesulfide (PPS), a semi-crystalline polymeric material, was the coating least susceptible to high-temperature hydrothermal oxidation in geothermal environments. Although early PPS coatings showed oxidation after exposure to acid brine at 392°F (200°C), they played a key role in successfully protecting inexpensive carbon steel heat exchanger tubes and test coupons against corrosion in wet, harsh geothermal environments (Gawlik et al. 1998, 1999, 2000, 2003, Sugama et al. 2001, 2003). Our findings suggested that PPS-coated carbon steel components could be used in place of expensive titanium alloys, Inconel, and stainless steels, which are frequently used in geothermal power plants.

Different filler materials can be added to the coating system to enhance surface hardness, thermal conductivity, and mechanical properties. The ceramic calcium aluminate (CA) has been shown to improve wear resistance and high-temperature stability of PPS coatings (Sugama et al. 2001). Adding carbon fiber to PPS improves both the thermal conductivity of the coating system and its mechanical properties. Depending on the application, fillers may be used to achieve a specific effect. For instance, in heat exchangers, high thermal conductivity and wear resistance are important, so a PPS coating system would use carbon fiber and CA fillers. In situations that do not involve heat transfer, such as well-field pipelines, the PPS system would use mostly CA as filler for wear resistance and high-temperature stability.

In a field test at the PGV plant, carbon steel tubes internally coated with PPS, applied by Curran International Corp., a commercial coating company, and carbon-fiber-reinforced PPS-coated coupons, made at BNL, were exposed for four weeks to injection geothermal fluid at a heat exchanger inlet temperature of 392°F (200°C), and outlet temperature of 180°F (82°C). Previous tests of coated tubes were performed at a maximum brine inlet temperature of 320°F (160°C), so this field test was the first one using the latest PPS formulations at a high temperature. The test was conducted in October 2003 and used uncoated carbon steel and type 2205 stainless steel tubes as controls. The results showed that the coatings resisted the high temperature brine, and scale did not adhere strongly to the coating, but the coating disbonded from the tube. Additional tests done at BNL found that coating failure was probably due to high residual alcohol levels in the slurry coating during the melt-flow procedure at 572°F (300°C). This is a failure mode that can be avoided with careful slurry application technique, or by the use of another technique, such as powder coating, that does not use alcohol.

## Test Method

The test skid installed and constructed by Thermochem at the PGV plant uses a side-stream of injection fluid at 392°F (200°C). Figure 1 is a diagram of the test skid. A total of 12 half-inch (13 mm) inside diameter, 20-foot-long (6 m) heat exchanger tubes are mounted in two shell and tube heat exchangers to simulate the conditions that would be encountered in vaporizer and preheater heat exchangers in a binary power plant using injection fluid as a heat source. Cooling water is supplied from the plant fresh water supply. Brine and coolant flows are instrumented to determine heat transfer and pressure drop performance of the tubes and a datalogger with modem allowed remote monitoring of the test. Two carbon steel tubes were coated internally with a commercially-applied PPS formulation developed at BNL. Two type 2205 stainless steel and two uncoated carbon steel tubes were also installed in both heat exchangers. In addition, carbon steel coupons coated with PPS at BNL were installed in pipelines carrying injection fluid in other areas of the PGV facility. Initial brine flow rates through the heat exchangers were set to obtain an average fluid velocity of 4 ft/s (1.2 m/s) in the tubes. The coolant flow rate was adjusted so that the brine outlet temperature of the preheater was in the range of ~180°F (~82°C). The test ran for 4 weeks, at which point a significant accumulation of scale was observed in the heat exchangers. At the end of the test, the tubes were removed from the heat exchangers, tested individually for heat transfer performance, weighed, and sectioned for further analysis at BNL and Thermochem.

## Results and Discussion

### Heat Transfer Performance

At the conclusion of the test, the heat transfer rates through the scaled walls of the tubes were individually determined using a single-tube heat exchanger. Calculation of the heat balance

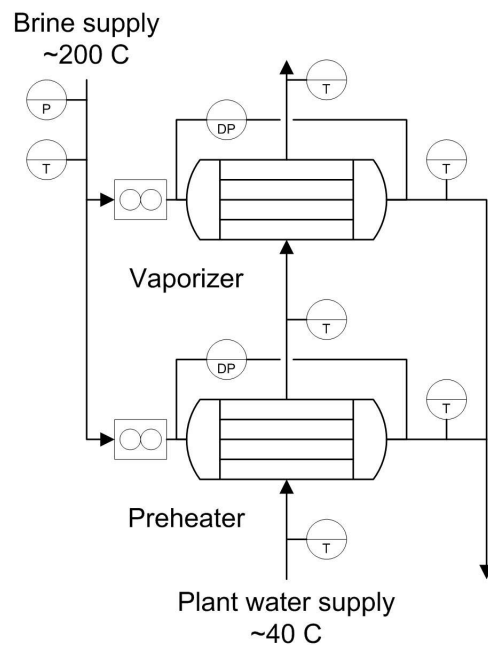


Figure 1. Schematic of the test rig at the PGV facility.

on the system yielded the coolant flowrate and average velocity, thus allowing the calculation of the heat transfer coefficient on the shell side based on standard relationships for turbulent flow. The overall heat transfer resistance was obtained from the heat balance, and when the exterior convective resistance and tube wall resistance were subtracted from the total, the interior heat transfer resistance was obtained. Comparing the interior heat transfer resistance in the new and exposed states indicates to what degree exposure to brine degrades heat transfer performance. Heat transfer deteriorates due to scale accumulation and the formation of corrosion products, and in the case of the commercially-applied coatings, lifting of the coating away from the tube wall, thus adding thermal conduction resistance.

The heat transfer results are summarized in Figure 2. The results for interior heat transfer coefficient,  $h$ , which consists of interior convection and conduction through the scale layer, after exposure are normalized with respect to performance when new. Three sets are shown in the figure—stainless steel (SS), PPS applied to carbon steel (CS/PPS), and uncoated carbon steel (CS)—for tubes that were installed in the vaporizer (vap) and preheater (pre) heat exchangers. The stainless steel tubes show a 35-46% drop in interior heat transfer rate with exposure. The uncoated carbon steel tubes show a 43-44% decline, while the coated tubes had a drop of 70%. The interior heat transfer coefficients for the SS tubes and CS steel tubes declined less in the preheater than vaporizer, consistent with the amount of scale deposited and the silica scale thermal quenching effect, as discussed later under Scale Thickness and Scaling Rates.

Although the coated and uncoated tubes experienced scale accumulations to varying degrees, the coating had largely disbonded, leading to significant additional heat transfer resistance. Disbonding was not observed for the PPS-coated

carbon steel coupons that were installed in injection brine pipelines. The coupons were coated by BNL, and the tubes by the commercial coating company, leading to the premise that application technique by the commercial coater was faulty. Failure mechanisms were explored by BNL and a likely cause has been found, as will be described below.

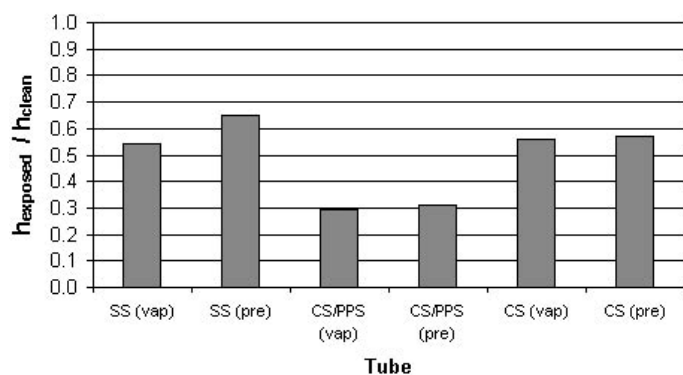


**Figure 2.** Heat transfer performance of the exposed tubes compared to new tubes.

### Post-Test Analyses

The analyses performed at BNL included the phase identification of scale deposited on the coating and stainless steel surfaces, the observation of how well scales adhere to the coating's and stainless steel's surfaces, and cross-sectional examinations of the coated coupons and lined tubes to obtain information on the corrosion-preventing performance of the coating and liner. Scanning electron microscopy (SEM) coupled with energy-dispersive X-ray spectrometry (EDX) and Fourier transform infrared spectroscopy (FT-IR) were used in the analyses. In addition, TCI performed X-ray diffraction (XRD) analysis of the scale deposits.

### Chemical Analysis of Scale

After the four-week-long exposure, we visually observed that the surfaces of the coated coupons and the CS/PPS and SS tubes' internal surfaces were covered with grey/brown scale. Also, we found that the scale could be easily removed from the coating surface by a conventional cleaning operation, such as hydroblasting, whereas the scale attached to the SS tubes was not easy to dislodge, reflecting an undesirable adherence. Figure 3 shows the SEM microphotograph and FT-IR spectrum, over the frequency range from 4500 to 500  $\text{cm}^{-1}$ , of the scales naturally flaked off from the coating's surfaces after drying them at 100°C. The SEM image revealed a dense, packed microstructure, representing some mechanical strength in the layers of scale.

To identify the chemical state of the scales, FT-IR analysis was performed on the 100°C-dried scale powder. The FT-IR spectrum (Figure 3) encompassed eight absorbance bands with assignments as follows (Farmer, 1964): at 3434  $\text{cm}^{-1}$ , revealing the stretching vibration of the hydroxyl (-OH) group and adsorbed moisture; at 2931 and 2861  $\text{cm}^{-1}$ , reflect-

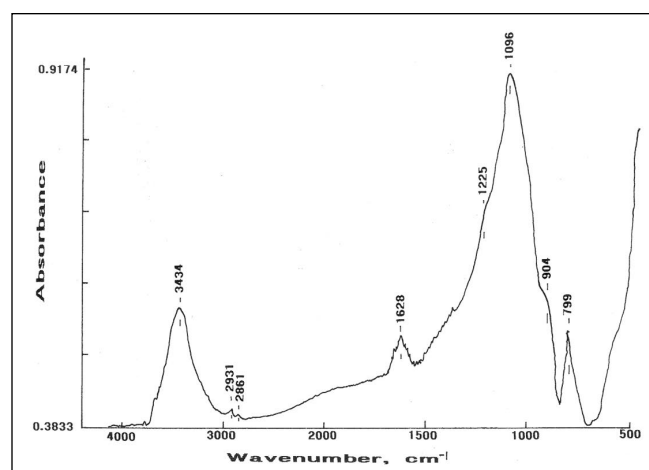
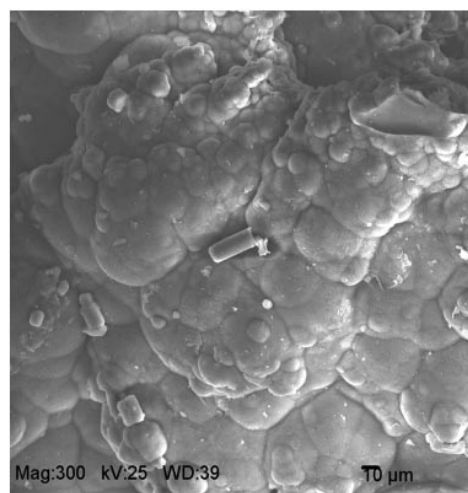


**Figure 3.** SEM microphotograph and FT-IR spectrum for scales deposited on the PPS coating applied to the coupons and carbon steel tubes, and also on the stainless steel tube surfaces after exposure for four weeks at PGV test site.

ing CH stretching vibration in the organic contaminants such oil; at 1628  $\text{cm}^{-1}$ , ascribed to the bending vibration of the H-O-H in adsorbed moisture; at 1225 and 1096  $\text{cm}^{-1}$ , corresponding to stretching mode of the Si-O band; and, at 904 and 799  $\text{cm}^{-1}$ , assigned to the bending vibration of the Si-O-H band. From integrating all these bands, we assumed that the scale is silica gel,  $\text{SiO}_2 \cdot x\text{H}_2\text{O}$ , with some oil contamination. The oil source was probably a petroleum-based corrosion inhibitor applied to the tubes before transport to Hawaii by ocean cargo.

An XRD analysis was performed on the scale from the SS tubes. The XRD spectrum (Figure 4, overleaf) shows the broad diffraction peak centered around 23° (2- $\theta$ ), characteristic of amorphous silica. The only crystalline phase detected in the sample was a trace of pyrite indicated by the 100% peak at 33° (2- $\theta$ ), and lesser peaks at 37.1° and 40.7°. The fact that no other heavy-metal sulfides deposited is significant for the application of a bottoming cycle at Puna, where such deposits have been known to occur and are difficult to treat. Amorphous silica scale, on the other hand, can usually be treated effectively by reducing the pH of the brine (pH-modification).

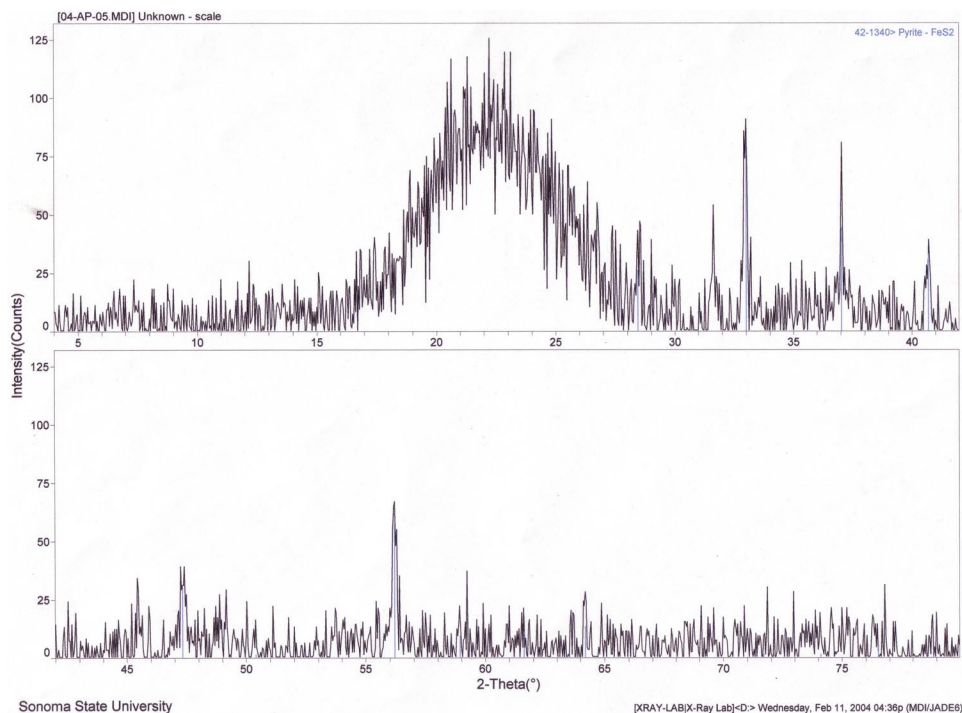


**Figure 4.** XRD spectrum of scale deposit from SS tube showing predominantly amorphous silica with traces of pyrite.

### Scale Thickness and Scaling Rates.

Figure 5 shows the SEM image of a cross-sectional area of a SS tube. Based on the SEM examination, the thickness of scale in this tube was about 8 mils (200  $\mu\text{m}$ ), so that the estimated rate of accumulation of scale was roughly 95 mils/year (2400  $\mu\text{m}/\text{year}$ ). Based on the weight gain for each tube and the scale density, the average thickness and rate of deposition was determined for all SS and CS tubes. The scaling rates for the SS tubes were 63 and 80 mil/yr (1600 and 2030  $\mu\text{m}/\text{year}$ ) for the preheater and vaporizer, respectively. For the CS tubes, the scaling rates were 77 and 117 mil/yr (1960 and 2970  $\mu\text{m}/\text{year}$ ) for the preheater and vaporizer, respectively. The carbon steel surface apparently enhanced the deposition rate of silica over that of stainless steel. This may be due to a greater presence of hydrated iron oxide corrosion products on the carbon steel surface. The tubes in the vaporizer had higher scaling rates than those in the preheater, even though the silica saturation index (S.I.)<sup>1</sup> was much higher in the preheater (S.I. = 2.0 vaporizer., 3.6 preheater). This difference is attributed to the thermal quenching effect on silica scaling kinetics. Rapid quenching of temperature reduces the kinetics of silica deposition and can enable the processing of high silica fluids through heat exchangers (Hirtz, 2000).

The quantity of scale deposited and the reduction in heat transfer after 4 weeks of operation is significant, but not unexpected. In fact, given the high level of silica supersaturation and fairly high salinity of the Puna brine, the results of this untreated baseline test are very promising. The next test at Puna will involve pH-modification, and the use of commercial scale inhibitors.

1. S.I. = actual silica concentration / silica solubility at given temperature.

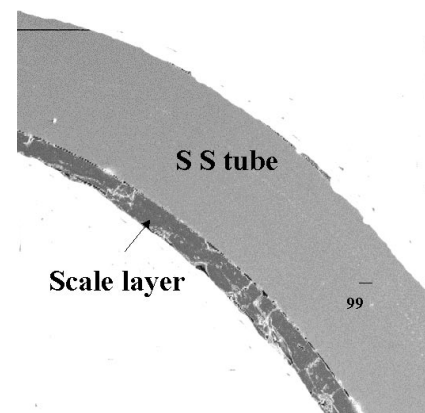


**Figure 5.** SEM image of massive scale layers deposited on an inner surface of stainless steel tube after only four weeks exposure.

### Stainless Steel Tube

Due to the strong adhesion observed between the scale and stainless steel surface, our interest shifted to investigating the mechanism of scale adhesion. To pursue this information, we explored the interfacial boundary region between the

scale layer and stainless steel by SEM coupled with EDX spectra (Figure 6). The SEM image clearly revealed that although there were some interfacial disbondments, the scales adhered well to the stainless steel's surfaces. The EDX spectrum taken from the interfacial area denoted as "A" had five chemical elements, O, Si, Cr, Fe, and Ni. Since the last three elements are associated with the stainless steel, the oxygen element not only comes from the silica, but also may originate from the Cr, Fe, and Ni oxides formed by the oxidation of stainless steel. If this interpretation is valid, the oxide layer occupying the outermost surface sites of the stainless steel may play an undesirable role in promoting its adherence to the silica scale. Further investigation of such interfacial boundary regions may explain the difference in silica scaling rates between carbon steel and other alloy materials.

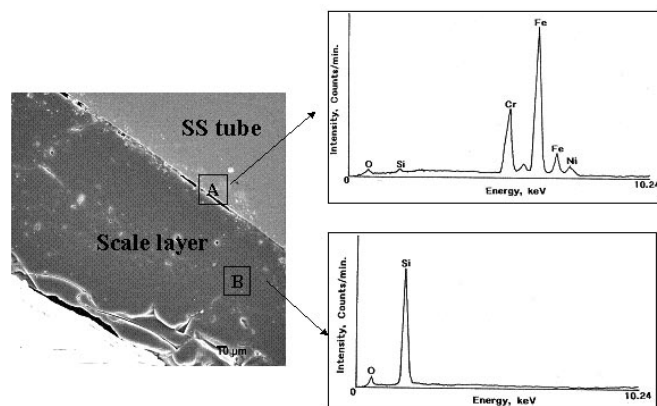


**Figure 6.** SEM close-examination coupled with EDX spectra at interfacial boundary regions between the scales and the stainless steel tube.

### PPS-Coated Carbon Steel Coupon.

The SEM image of a cross-sectional profile of the four-week-exposed coated coupon clearly verified that the coating remained intact (Figure 7). A close examination of the interfacial boundary region (Figure 8) highlights three distinctive layers: the PPS composite of around 80  $\mu\text{m}$  thick; the zinc phosphate (Zn.Ph) primer of  $\sim 12$  to  $\sim 17$   $\mu\text{m}$  thick; and the carbon steel. Also, there were no signs of delamination of the PPS coating from the Zn.Ph primer layer, as well as no obvious hydrothermal degradation. Thus, we were convinced that the PPS composite withstood hot brine at 200°C and adequately protected the carbon steel against corrosion. The EDX spectrum at the area “A” had three elemental peaks, S, C, and O, attributed to the carbon fiber-reinforced PPS composite. The EDX spectrum of the Zn.Ph primer layer, which acts as a link between the PPS coating and the steel, was characterized by three pronounced peaks related to P, S, and Fe elements, and weak C, O, and Zn signals. Since the S arises from the PPS, it appears that the PPS penetrated into the voids of the crystalline Zn.Ph layer during its melt-flowing process at 300°C and this anchored the PPS within the primer layer. This action of PPS is a very important feature in improving the interfacial bonding between the coating and primer. On the other hand, since the Fe element in the Zn.Ph layer comes from steel, we can assume that the primer layer not only consists of zinc phosphate compounds, but also includes iron phosphate compounds. Further, the incorporation of Fe into the primer layer led to the formation of a primer layer-embedded steel structure, underscoring the strong interfacial bonding between the primer and steel.

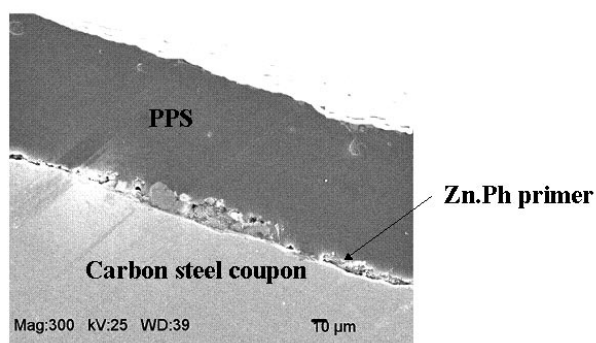


**Figure 7.** SEM image of cross-sectional area for carbon fiber-reinforced PPS composite-coated carbon steel coupon after exposure.

### PPS Composite-Lined Tube

Compared with the SEM image of the PPS composite-coated coupon made by BNL, the composite liner fabricated by Curran International Corp. exhibited a very rough surface, reflecting the liner's thickness, ranging from  $\sim 100$   $\mu\text{m}$  to  $\sim 530$   $\mu\text{m}$  (Figure 9). This thickness was much greater than that of the BNL coating ( $\sim 80$   $\mu\text{m}$ ).

One possible reason for the formation of such rough surfaces was an insufficient drying time for the isopropyl alcohol-based PPS composite slurry layers before the melt-flowing operation at 300°C. If any alcohol remains in the liner when

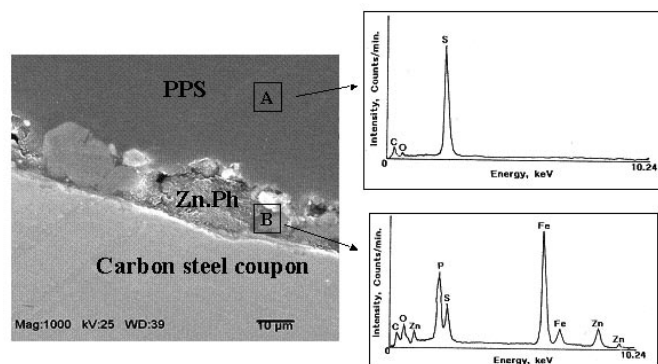


**Figure 8.** SEM image and the accompanying EDX analysis at interfacial boundary region between zinc phosphate-primed steel and PPS composite coating after exposure.

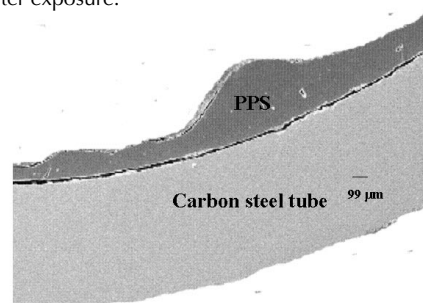


**Figure 9.** SEM image of cross-sectional profile for PPS composite-lined HX tube fabricated by Curran International Corp., after exposure.

melt flowing takes place, a rough surface texture is frequently created, and, further, the bonds to the underlying tubes become weaker because of the development of a porous microstructure in the composite layers due to the volatilization of the large amount of alcohol remaining in the slurry. To support this concept, we deposited 0.007 in.-thick (0.18 mm) composite liners in 0.5 in. (13 mm) diameter and 2-ft.-long (0.6 m) tubes. These liners were derived from slurries containing 0, 5, 10, 20, 50, and 80% alcohol, respectively, at 572°F (300°C). These composite layers were then subjected to the non-destructive wet sponge holiday test to detect pinholes and voids in the layers. All the liners made from slurries containing more than 20% alcohol failed this test. The wetting agent permeated through the failed liners, which had a rough and porous surface. This finding verified that the alcohol content of the slurry must be no more than 10% before baking it at 572°F (300°C) to produce smooth, non-porous liners. As expected, close examination (Figure 10) revealed that the PPS composite liner had delaminated from the tube's surfaces as one failure mode, and was evidenced in the poor performance of the liner in protecting the heat exchanger tube against corrosion. However, it is uncertain whether this delamination took place before or after the field test. The EDX spectrum at area “B” in the vicinity of the delaminated steel site included two intense peaks associated with the S and Fe elements, and the secondary peaks of C, O, and Zn. No P element was detected, clearly verifying that the tube has no zinc phosphate primer layer. It seems that the tube may have been galvanized before it was lined with PPS because we detected some Zn elements. From

the conspicuous Fe signal in conjunction with the O peak, this delaminated area appears to be occupied by corrosion products, such as iron oxides. However, there were no brine-related elements, such as Na and Cl in this area, seemingly suggesting that the liner did not allow the brine to permeate through it during the four-week-exposure. This finding can be taken as evidence that the PPS composite liner withstood hot brine at  $\sim 200^{\circ}\text{C}$ . Nevertheless, if our interpretation is correct that the primer used in this tube was a galvanized layer, the adherence of PPS liner to galvanized surfaces was poor because of their very smooth texture.

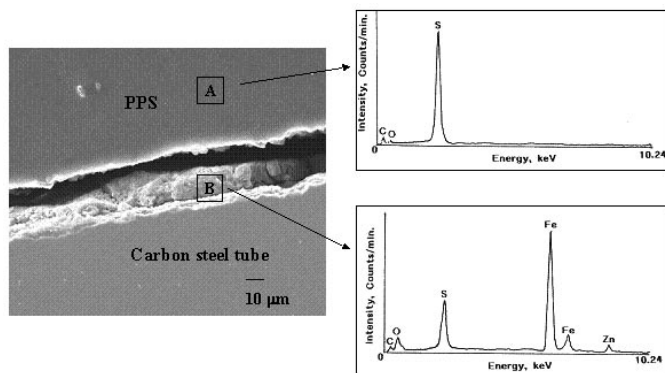


**Figure 10.** SEM image and EDX spectra at interfaces between the heat exchanger tube and PPS composite liner after exposure.

## Conclusions

Heat transfer performance results of all tubes exposed for four weeks to injection brine over a temperature range of  $\sim 200^{\circ}\text{C}$  to  $82^{\circ}\text{C}$  at the PGV facility showed a significant decline in overall conductance over the four-week test period. The coated tubes showed a larger drop than the uncoated tubes, due to disbonding of the coating. The decline in heat transfer was consistent with the amount of scale deposited in each tube. The scale was identified as amorphous silica with traces of pyrite. Scaling rates in the uncoated tubes ranged from 1600 to  $3000\ \mu\text{m}/\text{yr}$ , and were greatest in the carbon steel tubes. Scaling rates were lower at lower temperatures (within preheater), in spite of the higher silica saturation index, due to thermal quenching. The silica scale strongly adhered to the oxide layer on the surface of the stainless steel tubes. In

contrast to stainless steel, the surfaces of the microscale carbon fiber-reinforced PPS composite coating and liner were much more inert to scale deposition. In fact, the scales adhering to the composite surfaces were easily flaked off by hydroblasting. Although the exposure time was only four weeks, this composite coating and liner withstood hot brine up to  $400^{\circ}\text{F}$  ( $200^{\circ}\text{C}$ ). Thus, we believe that the PPS composite material has high potential as an anti-fouling and stable coating to  $200^{\circ}\text{C}$ . However, the improper fabrication of this composite lining system probably caused its failure by disbonding. This delamination was due to two reasons: One was the use of a galvanized primer, instead of the zinc phosphate primer; the other was the formation of a non-uniform, rough surface texture caused by the volatilization of a large amount of isopropyl alcohol remaining in the composite slurry during the melt-flowing operation of PPS at  $300^{\circ}\text{C}$ .

## References

- Farmer, V.C. and J.D. Russell, "The infra-red spectra of layer silicates", *Spect. Acta*, 20 (1964) 1149-1173.
- Gawlik, K., T. Sugama, R. Webster, and W. Reams, Sept. 22-23, 1998, "Field Testing of Heat Exchanger Tube Coatings," *Geothermal Resources Council Transactions*, v. 22, p. 385-391.
- Gawlik, K., S. Kelley, T. Sugama, R. Webster, and W. Reams, Oct. 17-20, 1999, "Field Testing of Heat Exchanger Tube Coatings," *Geothermal Resources Council Transactions*, v. 23, p. 65-69.
- Gawlik, K., T. Sugama, R. Webster, and W. Reams, 2000, "Development and Field Testing of Polymer Heat Exchanger Tube Coatings," *Geothermal Resources Council Transactions*, v. 24, p. 659-664.
- Gawlik, K., and T. Sugama, 2003, "Long-term Field Testing of Polyphenylenesulphide Composite Coatings," *Geothermal Resources Council Transactions*, v. 27.
- Hirtz, P., 2000, "Silica Scaling in Bottoming Cycles: Inhibition by Thermal Quenching". *Annual Geothermal Resource Council Meeting, Power Plant Operations and Maintenance Workshop*, lecture notes and study guide.
- Sugama, T. and K. Gawlik, Sept. 2003, "Self-repairing Poly(phenylenesulfide) Coatings in Hydrothermal Environments at  $200^{\circ}\text{C}$ ," *Materials Letters*, v. 57, p. 4282-4290.
- Sugama, T., and K. Gawlik, 2001, "Filler Materials for Polyphenylenesulphide Composite Coatings," *Geothermal Resources Council Transactions*, v. 25, p. 41-46.